Surface electronic structure of Ti-based transition metal alloys

S. E. Kulkova and D. V. Valujsky
Institute of Strength Physics and Materials Science, Russian Academy of Sciences, 634021 Tomsk, Russia

Jai Sam Kim, Geunsik Lee, and Y. M. Koo
Department of Physics, Pohang University of Science and Technology, Pohang 790-784, Republic of Korea
(Received 10 November 2000; revised manuscript received 19 April 2001; published 6 February 2002)

The electronic structure of the (001) and (110) surfaces for $B2$ Ti-based transition metal alloys were investigated using the full-potential linearized augmented plane-wave method in the local-density approximation. The evolution of the electronic structure of alloys at the different surfaces in comparison with the bulk ground states is analyzed. The ferromagnetic order is displayed in the case of Fe or Co top layer for the (001) surface. The surface magnetic moment of Fe and Co ($2.27\mu_B$ and $0.87\mu_B$) reduces drastically inside the film. The influence of a surface on the electron properties of alloys is discussed.

DOI: 10.1103/PhysRevB.65.085410 PACS number(s): 71.20.Be, 73.20.At

I. INTRODUCTION

Since the discovery of the shape memory effect (SME) the attention of the researchers has been attracted to binary transition metal alloys, which exhibit a martensitic phase transformation accompanied by SME. Shape memory bulk Ti-based alloys have been the subject of intensive experimental and theoretical investigations.[1–17] Most of them crystallize in $B2$ structure at higher temperature. It transforms martensitically to a monoclinic phase (TiNi) or an orthorhombic one (TiPd, TiPt) upon cooling. The martensitic transformations (MT's) in the nearly equiatomic alloys are significantly affected by the addition of the third element as regards the MT temperature and crystal structure. The mechanism of MT in shape memory alloys is related to the peculiarities of their electronic structure (ES).[6–14]

Among the alloys showing SME TiNi is the best known example.[1–4] SME of TiNi was at a focus of a number of works due to the convenient transformation temperature of 333 K. This material, also called nitinol, has been used in the aerospace industry, for electronics and mechanical engineering. In the last decade TiNi-based alloys have found widespread applications in medicine also. In this context the study of biocompatibility[15–17] of alloys is an especially important task. In the case of TiNi the knowledge of the nature of its biocompatibility is very important because Ti is a good implant material but Ni is well known as a hazard material.[18] However, biocompatibility is the surface related property. Until recently virtually nothing was known about ES of the Ti-based alloy surface. Basically surface ES for different transition metals (TM's) or a monolayer of TM on an inert substrate was investigated.[19–24] There exist a few papers where the transition metal alloy surfaces were investigated.[24–29] The (001) and (110) surfaces were studied very intensively for $B2$ NiAl alloy.[30–34]

The knowledge of surface electronic structure for transition metal alloys is also important for understanding the martensitic transformations at the surface, which can be different from those in the bulk. Adsorption on the ordered transition metal surfaces is a rather unexplored field yet.[32,34] In order to explain structural, electronic, magnetic, biological, and biochemical properties in TM alloys at the microscopic level we need to thoroughly understand the electronic structures of their clean surfaces.

In this paper, using the full-potential linearized augmented plane-wave (FLAPW) method,[35] we focus on ES calculation for the (001) and (110) surfaces. We have performed a comparative study of the surface electron structure in the TiFe-TiCo-TiNi series. The corresponding ES changes and the alteration of electron properties at the surface are discussed.

II. CALCULATIONAL DETAILS

The electronic structure for bulk $B2$ TiMe (Me=Fe, Co, Ni) as well as TiMe (001) and (110) surfaces were calculated using the WIEN97 implementation[36] of the FLAPW method within local-density approximation (LDA) for the exchange-correlation potential. Using the supercell technique, the surface was simulated by repeated slabs separated by a vacuum region in the z direction. The thickness of the vacuum region corresponding to three bulk lattice spacings was found to be sufficient to avoid interactions of the Ti(Me) atoms. The lateral lattice parameter was set to experimental lattice constant for the bulk alloys (2.976, 2.99, and 3.015 Å (Ref. 37) for TiFe, TiCo, TiNi, respectively). The equilibrium lattice parameters obtained from a nonrelativistic calculation within LDA are 0.5–1% smaller than the measured ones. The volume behavior and bulk moduli for bulk TiMe alloys were studied in detail in our previous papers.[6] The core states were treated in a nonrelativistic fashion. The $3s$ and $3p$ states were treated as the valence-band states. The multipole expansion of the crystal potential and electron density inside the muffin-tin spheres was cut at $l_{max}=10$. Nonspherical contributions to charge density and potential within muffin-tin spheres were considered up to $l_{max}=4$. In the interstitial region the charge density and the potential were expanded as a Fourier series with wave vectors up to $G_{max}=10$ a.u.$^{-1}$. The plane-wave cutoff was 4 a.u.$^{-1}$. The muffin-tin radius was 2.3 a.u. for all components of alloys but the smaller value of 2.0 a.u. was used in the relaxation process. The electron energy spectrum was calculated at 165 **k** points in the irreducible part of the Bril-

louin zone (IP BZ) for the bulk $B2$ phase. The extensive convergence tests were performed with respect to the **k**-point set and energy cutoff for the basis set for five- and seven-layer TiNi slabs. Our simulation showed that a five-layer slab makes a good approximation of the (110) TM alloy surface but a seven-layer slab must be used for the (001) surface. Finally the electron energy spectrum was calculated at 72 **k** points in the irreducible part of the two-dimensional Brillouin zone (2DBZ) for the (001) surface and at 24 **k** points for the (110) surface. The energy cutoff was the same as in the bulk calculations (15.6 Ry). Self-consistency was considered to have been achieved when the total-energy variation from iteration to iteration did not exceed 5×10^{-4} Ry in the surface calculation. The calculated density of states (DOS) was broadened by a Gaussian function with a width of 0.2 eV to suppress noise. An electron state is considered a surface state (SS) if more than 80% of its probability is located in the surface (S), subsurface (S-1) layers, and the vacuum region.

The simplest variant of the surface for $B2$-TM alloys is the (001) surface, which consists of alternating metallic monolayers of Ti or Me. The idealized TiMe(001) surface can be terminated by either Ti or Me atoms. There is no experimental data on the relative stability of these two surface terminations. In the present paper both Ti and Me terminations of the TiMe(001) surface are considered. These variants are denoted by Ti/TiMe and Me/TiMe, respectively. Another interesting surface in $B2$-TiMe alloy is the (110) surface. In this case each layer is a rectangular lattice consisting of Ti and Me atoms with the same stoichiometry content as the bulk alloy.

We have also investigated whether our surfaces are truthfully simulated: we check if the central layers properties coincides with those of the bulk. Comparison of the local-density of states (LDOS) for the central layer (C) and the first from center layer (S-2) and their sum with the corresponding local and total DOS of bulk alloy showed that the bulk region is reasonably well reproduced in the surface calculations. In addition, the properties of the central layer were found to coincide quite well with those of the bulk alloy.

III. RESULT AND DISCUSSIONS

A. (001) surface

Figure 1 shows the calculated LDOS for the seven-layer Ti/TiNi(001) and Ni/TiNi(001) films. A significant change in the surface LDOS compared to that for S-2 ''bulklike'' layer is observed for both surface terminations. As seen in Fig. 1 the effect of the surface is dramatically confined to the surface layer, however, it is already much weaker in the subsurface layer. The ES changes are more significant for the Me-terminated TiMe(001) film and result in sharp peaks below the Fermi level (E_F). In the Me/TiMe cases the ES changes rapidly diminish in the depth of the film, whereas for the Ti/TiMe they are less significant but more pronounced inside the film. Me resonance surface states are concentrated in a rather narrow energy interval below E_F and their shifts towards E_F from -1.5 eV in Ni/TiNi up to -0.3 eV in Fe/TiFe are observed. Ti SS's are located in the

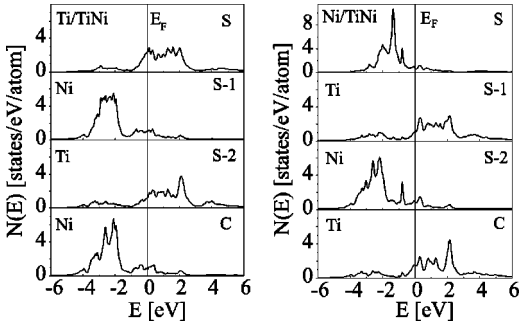

FIG. 1. LDOS for both terminations of seven-layer TiNi(001) film. The labels C and S mark the central and surface layers, respectively. The labels S-1 (subsurface) and S-2 correspond to the position from the surface.

vicinity and above E_F. The valence bandwidth decreases from 7.30 eV in bulk TiFe down to 6.75 and 6.62 eV for Ti/TiFe and Fe/TiFe, respectively. The surface bandwidth slightly increases for TiCo (6.95 and 6.84 eV) and TiNi (7.06 and 7.05 eV). The change in ES is related to the charge redistribution near the surface and the appearance of the surface states. The analysis of the *s*-, *p*-, *d*-contributions to the charge density for different layers shows that the charge density tends to increase towards the central layer for both surface terminations. The charge decrease in the surface layer is due to the reduction in the number of the nearest neighbors at the surface (in the bulk each atom has eight nearest neighbors, whereas on the (001) surface an atom has only four). This results in the delocalization of *s* and *p* states at the surface and the charge redistribution in the interstitial and vacuum regions. The decrease of the valence charge is mainly due to *p* electrons. *Me d* orbitals are more localized within muffin-tin spheres than those of Ti. The splitting of the states together with the dehybridization between *s*-*p* and *d* states takes place at the surface of the transition-metal alloys as it was also noted earlier for pure transition metal.[17–21]

The energy bands along the symmetry direction of the 2DBZ for all considered alloys (Me terminated surfaces) are shown in Fig. 2. The dispersion curves for TiNi are in a good agreement with those[33] obtained by the film LAPW method. To determine surface bands we selected the states which had more than 80% occupation probability in the surface, subsurface layers, and the vacuum region. The changes of this criterion down to 60% can lead to the expansion of the surface states region. In this case the states are divided further into ''weak'' and ''strong'' surface states. Namely, strong surface states are shown by the dark filled circles in Fig. 2. All of the surface states are basically of *d*-type symmetry and only a few of them contain insignificant portions of *s* and *p* symmetry. This conclusion follows from detailed analysis of SS orbital composition and a degree of the localization in the surface and subsurface layers at all symmetry points of the 2DBZ. On both Me- and Ti-terminated surfaces there are many so-called Tamm surface states,[38] which are pulled out of the bulk *d*-band continua. They are due to perturbation of the crystal potential at the surface (by bulk/surface potential shift). There are also the Schockley SS's,[39] states that resemble ''dangling bonds,'' which are located in the bulk

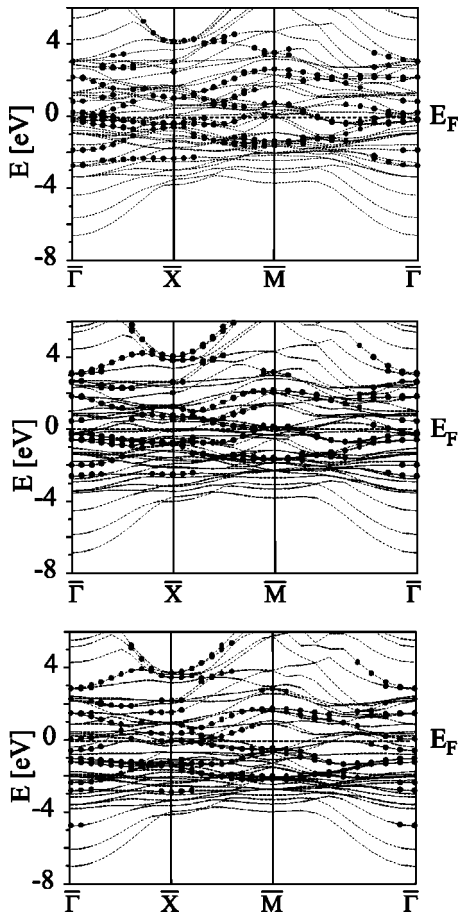

FIG. 2. Electron energy spectrum $E(\mathbf{k})$ for Fe/TiFe, Co/TiCo, and Ni/TiNi (001) films, respectively, the dark filled circles represent the surface states.

band gaps. For example, in Fe/TiFe the occupied states near E_F at the Γ point can be associated with the Tamm SS, whereas the lowest states at the Γ point are Schockley SS. Unfortunately it is impossible to classify all SS's within the framework of the simplified Tamm-Schockley scheme,[38,39] which was used often in the literature for pure transition metals.[19] The majority of surface states observed in the Ti/TiMe(001) film are also present in the Me/TiMe(001) film, though they are located low in the energy scale. In general, main peaks of LDOS for both TiMe (001) surface terminations are due to the same states, which are characteristic of bcc transition metal (001) surface.

An increase of density of states at the Fermi level $[N(E_F)]$ in the surface layer is observed in all Ti-terminated TiMe(001) films considered. $N(E_F)$ changes from 1.22 (S-2 layer) up to 2.49 states/eV/atom (S-layer) in Ti/TiNi. It should be noted that $N(E_F)=1.23$ states/eV/atom in the bulk TiNi. $N(E_F)$ for Ni-terminated film is smaller than that in bulk. It is known that the knowledge of the states near E_F is very useful for understanding the chemical reactivity at the surface. Our calculations show that most of the surface states near the Fermi level are Ti states. Besides the surface states for the Ti-terminated surface extend into vacuum region deeper than for the Me-terminated surface. The present results indicate that the Ti atoms at the surface possess a higher

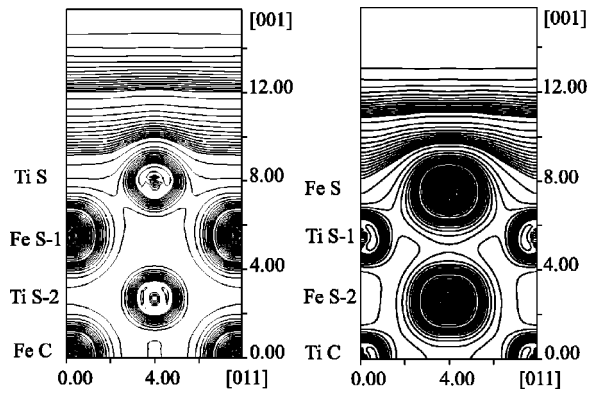

FIG. 3. A contour plot of the charge-density distribution in a [011] plane perpendicular to the (100) surface after relaxation process for Ti/TiFe and Fe/TiFe (001).

reactivity than the Ni or Co atoms. This can explain the presence of the titanium oxide film at the TiNi surface.[16] Therefore the Ti-terminated TiMe(001) surfaces cannot be inert. It should be pointed out that SS in the Fe-terminated TiFe(001) film are located more closely to E_F. In this case both Fe and Ti atoms at (001) surface possess a high reactivity. The larger density at the Fermi level is typically considered an indication for a more unstable system. Actually the presence of many SS's near the Fermi level for the Ti-terminated TiMe(001) films also indicates the possibility of the surface reconstruction.

We estimated the work function (ϕ) for the TiMe(001) systems considered. The obtained values of the work function are 5.1–5.3 for Ti/TiMe and 5.3–6.0 eV for Me/TiMe, respectively. The change of the work function with respect to the metal charge correlates well with theoretical and experimental results for pure Fe, Co, and Ni (5.04–5.53 eV).[40] So, the work function depends more significantly from the top layer atomic characteristics than from the film composition.

We estimated the relaxation in the case of TiMe(001) surface. The geometry optimization has been performed for Ti/TiFe(001) and Fe/TiFe(001) systems only. The Hellman-Feynmann forces were used for the geometry optimization. Unfortunately, a complete relaxation of the TiMe(001) system remains a formidable computational task. The calculation of forces is very critical with respect to cutoff parameters. The lateral parameter was fixed at the experimental lattice parameter. The interlayer distances were optimized with a damped Newton dynamics. The relaxation ($\Delta d_{ij}/d_0$, i, j are layer numbers) was calculated with respect to the interlayer spacing $d_0=1.488$ Å. Within the LDA we found a surprisingly strong contraction of the interlayer distance between the surface and subsurface layers, -25.6% for Fe/TiFe and -13.9% for Ti/TiFe, whereas the second interlayer distance expanded by 1.5% in both cases. These values did not change significantly when the two innermost layers were fixed at the bulk coordinates. A contour plot of the charge-density distribution in a plane perpendicular to the surface and extending along [110] direction is shown in Fig. 3 for both terminations of the TiFe(001) film after the relaxation process. Ti surface states are distributed deeper in the vacuum region in comparison with Fe SS's. The interaction

is stronger along the direction of the nearest-neighbors atoms in Fe/TiFe(001) film and the covalent bond is formed in this case.

We can compare the calculated relaxation of the interlayer distance with the results for pure transition metal or for TM on a Cu substrate only. Strong relaxation for two monolayers of Co and Mn on Cu(001) substrate (-17.0% and -30.86%, respectively) were also obtained in Refs. 23 and 24. Similar behavior was reported recently for nonmagnetic Fe(001) film,[25] where the values of $\Delta d_{12}/d_0 = -20.7\%$ and $\Delta d_{23}/d_0 = 9.5\%$ were found using the FLAPW method with the generalized gradient approximation (GGA) (Ref. 41) for the exchange-correlation potential. In the case of V(001) the relaxation of the first interlayer distance is -11.1%.[30] A recent projector augmented wave (PAW) calculation[27] of V(001) also found relaxation of -13.6% and 1.0% for the first two interlayer distances. In this respect we think that our values are reasonable although we feel the criticism results because the values are very large in comparison with experimental ones in the case of pure transition metal. It should be noted that the choice of the lateral parameter can also influence on the value of the first interlayer distance.[23] In any case one needs to expect much larger values of the relaxation for TM alloys. As follows from results obtained, for example, in Ref. 24, the magnetism pushes the relaxation back and only a small inward relaxation of -0.6% remains for Fe(001). In Ref. 25 outward relaxation of 3.37% (3.63%) was obtained for the antiferromagnetic and ferromagnetic 2-monolayer (ML) Mn/Cu(001) system. At the same time the influence of magnetism was less in 2-ML Co/Cu(001) where the value of -13.4% was found.[23]

B. Magnetic properties

It is well known that if the surface of the material consists of ferromagnetic atoms, there is a magnetic moment at the surface even though it is absent from the bulk state. Experimental and theoretical investigations indicate that the magnetic moment is enhanced as compared to the bulk value in the magnetic system. Since iron is known to be a good magnetic metal, we also investigated the possibility that a ferromagnetic surface layer forms in the Fe/TiFe(001) film. Similar investigations were also made for Co/TiCo(001) and Ni/TiNi(001). To achieve this we performed spin-polarized calculation within LSDA. The local spin densities of states for Co/TiCo and Fe/TiFe are shown in Fig. 4. In general, the results show similar trends to those observed for the nonmagnetic cases. The LDOS structure of the central layer differs insignificantly for the majority and minority spin for Fe/TiFe and Co/TiCo (001) films but we find significant differences in the surface layers. The exchange splitting of the states with opposite spin and the narrowing of the *d* bands results in the appearance of the magnetic moment at the surface. We estimated the layer-resolved magnetic moments for both systems considered. It was found that the Fe-terminated film exhibits a slight enhanced magnetic moment $2.27\mu_B$ [$2.272\mu_B$ (Ref. 26)] compared to the Fe bulk value ($2.22\mu_B$), whereas Co has a reduced value of $0.87\mu_B$ in comparison with that for bulk Co ($1.72\mu_B$). It is also less

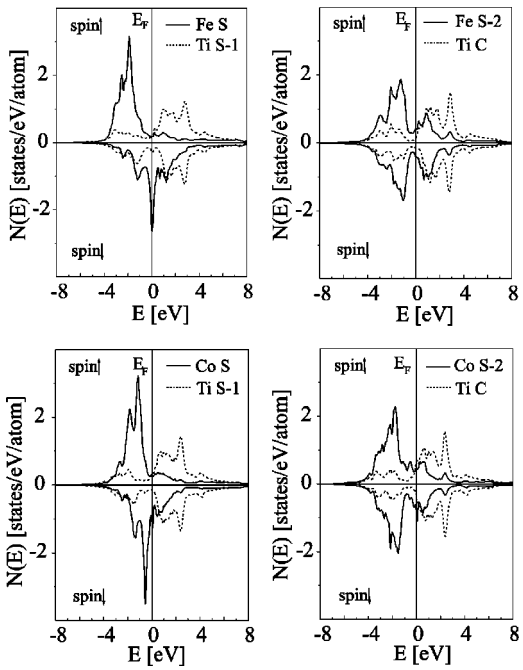

FIG. 4. LDOS of the different layers for magnetic Fe/TiFe and Co/TiCo (001) systems. *Me* bands are marked with solid lines and Ti bands with dashed lines.

than that obtained for Co on the copper substrate (1.71–$1.78\mu_B$).[23] This is the contribution from the muffin-tin region only because the interstitial region contributes only a little.[26] The contribution of *s* and *p* electrons to the total moment is insignificant. To the best of our knowledge magnetic moments for Fe or Co terminated TiMe(001) surfaces have not yet been measured. The calculation for the Ni/TiNi (001) surface reveals that it is not magnetic at all. The magnetic moment of Fe and Co atoms decreases significantly inside the films, having diminished to 0.41 and $0.32\mu_B$ by the first from center layer, respectively. The reduction of the magnetic moment for pure TM in the subsurface layers was also noted in Refs. 22–26. We note that the same trend of an enhanced magnetic moment in the surface layer ($3.85\mu_B$) and a reduced magnetic moment in the subsurface layer ($3.40\mu_B$) was also found in our previous FLAPW calculation for NiMn(001). The reduction of the Mn magnetic moment is much smaller than in above-mentioned cases of Co and Fe. As a consequence of the exchange splitting at the surface the Fe (Co) states of electrons with spin down are displaced relative to those with spin up on the energy scale. These states overlap significantly with Ti states. This is the reason for magnetic oscillation inside the film in TiMe(001). For detailed investigation of the oscillation of the magnetic moment in the plane perpendicular to the surface (the spin-density-wave formation) it is necessary to consider much thicker film.

Our result reveals also that the magnetic moment of Ti in the subsurface layer is negative ($-0.41\mu_B$ and $-0.18\mu_B$ in TiFe(001) and TiCo(001), respectively). M. Talanana *et al.*[29] obtained a similar result for the $B2$ FeV(001) surface. The induced magnetic polarization on the V atoms at the Fe-V interface was reported in numerous experimental and theo-

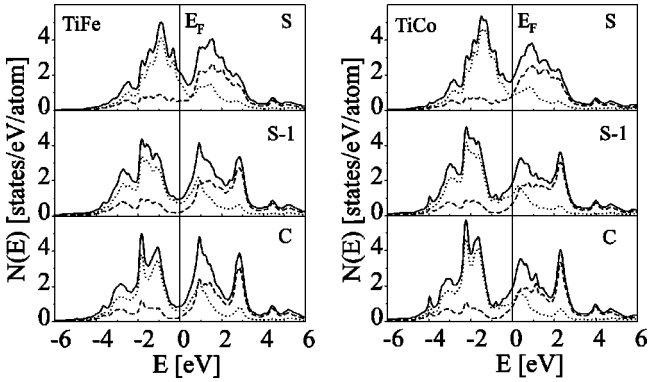

FIG. 5. Total and local DOS for five-layer TiFe and TiCo (110) films.

retical investigations also.[22,26,29] In the present paper the values of magnetic moments are given for nonrelaxed surfaces. Probably the strong relaxation of the interlayer spacing for magnetic Fe/TiFe and Co/TiCo films will take place also as in Ref. 23. It has a noticeable effect on the magnetic moments and cannot be neglected. The calculations are being performed now and will be presented together with the results of the hydrogen adsorbtion in these alloys in our forthcoming paper.

The values of the work function for magnetic Fe/TiFe and Co/TiCo systems (4.4 and 4.6 eV) are less than obtained for the nonmagnetic case (5.3 and 5.8 eV). The present results for the Me/TiMe(001) surface allow us to draw the conclusion that the magnetic order for the Fe- and Co-terminated TiMe(001) films is energetically favorable. The energy differences between ferromagnetic and nonmagnetic configurations equal to -0.86 and -0.64 eV is found for Fe/TiFe(001) and Co/TiCo(001) systems, respectively.

C. (110) surface

The (110) surface of $B2$ alloys has received greater attention in past studies, which mostly examined NiAl.[30–34] Our calculation shows that a five-layer slab already reproduces the surface and bulk region quite well. We would like to emphasize that the surface effects are confined mainly to the surface layer in the case of the (110) surface, and do not spread into solid (top panel in Fig. 5). This is in consistent with the short screening length in transition metals. The influence of the surface decreases faster in the (110) film because its interlayer spacing is greater than that in the TiMe(001) film ($d_{110}=\sqrt{2}d_{001}$). The DOS difference between surface and subsurface layers is enormous. The displacement of the center of gravity of the d bands towards E_F is less than that on the (001) surface. The decrease of charge observed in the surface layer of all investigated alloys is mostly due to s and p electrons (10^{-2} electrons), whereas the change in charge due to d electrons is an order of magnitude less (10^{-3} electrons). Analysis of different charge contributions (dt_{2g} and de_g) indicates covalent binding at the (110) surface. The detailed analysis of the surface states confirms this fact. The bond decreases insignificantly in comparison with bulk alloys, which is ascribed to the presence of different atoms in the layer, and to the smaller distance between atoms within one layer in TiMe(110). Note that the (110) surface is the most close packed in the bcc structure. The coordination number of the nearest neighbors is 6 (it is 8 in the bulk). As in TiMe(001) surfaces, the Me states change more in the surface layer than those of Ti. The congruence of the maxima of Fe and Ti differences between surface and subsurface LDOS indicates the strong hybridization of the surface states. In general, the surface ES has similar features to those in the bulk. Basically a redistribution of the states into d subbands is happening. Moreover, there is no large splitting into subbands connected to t_{2g} and e_g symmetry in the surface layer, as is in the bulk.

The Fermi level shifts in the region of the ''bonding'' states in TiFe(110), whereas it lies in the deep minimum between two main DOS peaks for the bulk alloy. The density of states at the Fermi level [$N(E_F)=2.27$ states/eV/cell] increases in comparison with the bulk (0.39 states/eV/cell). The situation is opposite for TiCo(110) film, where the Fermi level lies in DOS minimum and $N(E_F)$ is lowered in comparison with bulk. A significant increase of $N(E_F)$ is observed for TiNi(110) film. It is known that the relatively high chemical activity of the transition metals and their alloys is caused by a high DOS at the Fermi level and in its vicinity. As follows from the present results TiNi and TiFe differ slightly from a typical $3d$ transition metal and their clean surfaces (110) cannot be inert. In addition it should be noted that the surface might strongly affect the phase transformation in TiNi with respect to the martensitic transformation temperature.

The calculated values of the work function are 5.2, 5.1, and 4.9 eV for TiFe-TiCo-TiNi (110) surfaces, respectively. The obtained values exceed the corresponding ϕ values for clean TM surfaces. The similar behavior was noted for NiAl (110) also.[40] The ϕ values obtained for the (110) surface are less than those for both terminations of the (001) surface contrary to pure transition metals. The metal work function for the (110) is larger than that for the (001) surface.

D. Electron properties

We also studied the influence of a surface on the electron properties for the nonmagnetic TiMe(001) system. The theoretical x-ray spectra were calculated taking into account the matrix element, which were multiplied with a radial transition probability and the partial densities of states. They were smeared with a spectrometer function of half width 0.6 eV. The lifetime broadening with a Lorentzian of half width 1 eV was also applied to the curves. The calculated x-ray K, L-emission and absorption spectra for TiMe(001) film show insignificant change in comparison with the bulk spectra. For example, the change of TiFe LDOS at the surface results in appearance of the finer structure near the Fermi level for both surface terminations (Fig. 6). The narrowing of the d band at the surface leads to decrease of $K\beta_{25}$ line in all alloys considered. As the absorption spectrum reflects the states above E_F, the difference in the splitting of d band into e_g and t_{2g} subbands exhibits in the width of the selective line. This feature is more pronounced for the Ti spectrum, which

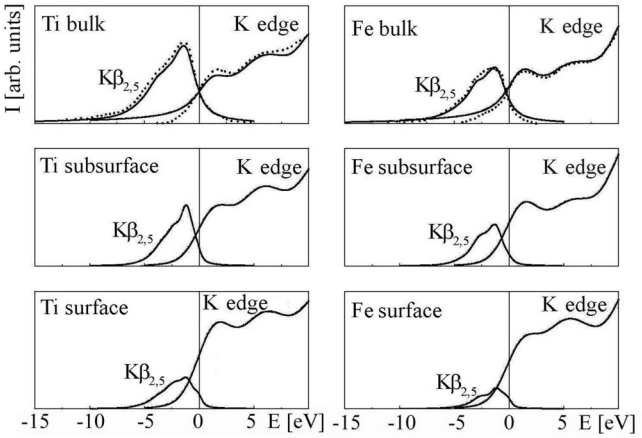

FIG. 6. Ti and Fe *K*-emission and absorption spectra in the central, subsurface, and surface layers for TiFe (001). The points represent experimental data from Ref. 42.

agrees well with LDOS of alloy. The emission and absorption spectra obtained for central layers of all TiMe(001) films agree quite well with those for bulk alloys and experimental ones (Fig. 6).[42] This fact confirms fast damping of the surface perturbations into solid. Calculations of the electron energy-loss spectra L_{23} as well as x-ray-absorption spectra showed an increase of absorption on the different surfases of the TiFe(001) film in comparison with the bulk, whereas for the TiNi(001) and TiCo(001) films the absorption increases only for the Ti-terminated film.

The optical conductivity spectra $\sigma(E)$ for the TiMe(001) thin film are shown in Fig. 7. Only the interband contribution to $\sigma(E)$ is given in Fig. 7. It is known that the effect of the intraband transition is significant up to 0.5 eV. Our calculations for bulk alloys showed that the theoretical intraband curves have no fine structure. Besides, the intraband contribution gives the rise of $\sigma(E)$ for $B2$ bulk TiCo and TiNi in above mentioned region. The obtained optical spectra for bulk TiMe alloys are in good agreement with experiment.[3,43,44] Figure 7 shows that $\sigma(E)$ obtained for the Ti-terminated TiNi(001) and TiCo(001) are very close to the theoretical $\sigma(E)$ curves for bulk alloys. Moreover, they reproduce well the experimental peaks[3] in the infrared region

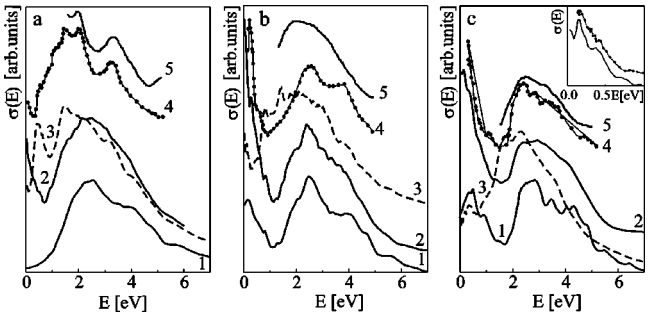

FIG. 7. Optical conductivity $\sigma(E)$ of TiMe (001) thin films, where Me=Fe, Co, Ni: curve 1 is $\sigma(E)$ for bulk $B2$ TiMe, curves 2 and 3 are $\sigma(E)$ for Ti- and Me-terminated $B2$ TiMe (001), curve 4 is the experiment from Refs. 3 and 43, curve 5 is the experiment from Ref. 44, respectively.

[the inset to Fig. 7(c)], which we could not obtain using "bulk" electronic structure for TiNi.[6] The optical spectra for the Me-terminated film are shifted towards E_F and they differ significantly from those for bulk alloys. Both theoretical curves for TiFe(001) reproduce the increase of $\sigma(E)$ near the Fermi level, which is due to the shift of E_F from the dip in DOS in the surface calculation. $\sigma(E)$ for Ti/TiFe(001) has no minimum between the peaks in the visible part of the spectrum as in the bulk TiFe. The spectrum for the Fe- and Co-terminated (001) surface shows the fine structures observed in experiment[43] in the low-energy region. In general, the influence of the surface is less pronounced in the case of the Ti-terminated TiCo and TiNi(001) films but it is substantial for the Me-terminated films. In addition, the results obtained for the Me-terminated films suggest that the fine structures in the optical conductivity curves in the low-energy region are mainly due to the Me contribution.

IV. SUMMARY

We performed FLAPW calculations of electronic structures for the (001) and (110) surfaces of the TiFe-TiCo-TiNi alloys and studied the change of the electron characteristics at the surface. Significant changes in the electronic structure near the Fermi level on both (001) and (110) surfaces are observed in all alloys investigated. In the case of TiFe(001) surface the presence of the resonance surface states near the Fermi level is found for both Ti- and Fe-terminated films. This indicates that the TiFe(001) surface possesses a high reactivity. An investigation of the hydrogen adsorption in this key material for hydrogen storage needs to be carried out for both surface terminations. The increase of LDOS at the Fermi level for the Ti-terminated TiMe(001) films can be an indication of the high reactivity of Ti atoms and can explain the presence of the titanium oxide film on the surface for the TiNi-based alloys. The presence of the surface states near the Fermi level can cause a reconstruction of the Ti-terminated (001) surface in these alloys. The electronic structure of the (110) surface has similar features as those in the bulk. A redistribution of the states into d subbands is generally observed on the surface for all TiMe alloys. The result obtained for the TiFe and TiNi(110) film predict their instability, whereas the TiCo(110) film seems to be more stable in comparison with the bulk alloy.

The ferromagnetic order is observed in the case of the Fe and Co top layer for the TiMe(001) surface. The Fe and Co surface layers exhibit magnetic moments equal to 2.27 and $0.87\mu_B$, respectively but they diminish fast inside the films. A small-induced polarization of the subsurface Ti atoms $(-0.41\mu_B)$ occurs. The absence of the magnetism found for the TiNi(001) surface reflects the physical reality. In general, the ferromagnetically ordered systems are lower in energy than the nonmagnetic ones.

The calculated L electron energy-loss spectra show the increase of the absorption on both surface terminations of the TiFe(001) film, whereas in TiNi and TiCo the absorption increases only for the Ti-terminated (001) films. The calculations of the optical conductivity spectra show that the influence of the surface is less pronounced for the Ti-

terminated TiMe(001) films but it is substantial for the Me-terminated films. Moreover, the obtained results suggest that fine structures of the optical conductivity spectrum in the low-energy region are basically due to the Me contribution. Our interpretation agrees quite well with a strong dependence of the low-energy peaks on metal Fe (Co) concentration observed in Ref. 43. We hope that the present paper will stimulate the experimental investigation of the optical properties for the transition-metal alloy thin films.

At the present time the nature of good biocompatibility of TiNi is related to its tendency to be covered by titanium oxide. The present result can be also the base for studying initial oxidation of the Ti-terminated TiNi(001) surface.

ACKNOWLEDGMENTS

This work was partly supported by a collaborative program between the Institute of Strength Physics and Materials Science of RAS, Tomsk, Russia and the Basic Science Research Institute, Pohang University of Science and Technology, Republic of Korea. It was jointly funded by the KOSEF-2000 research fund also.

[1] F. E. Wang, W. J. Buehler, and S. J. Pickart, J. Appl. Phys. **36**, 3232 (1965).
[2] P. M. Ossi and F. Rossitto, J. Phys. F: Met. Phys. **11**, 2037 (1981).
[3] S. A. Shabalovskaya, Phys. Status Solidi B **132**, 327 (1985).
[4] V. G. Pushin, V. V. Kondrat'ev, and V. N. Khachin, Sov. Phys. J. **28**, 341 (1985).
[5] D. A. Papaconstantopoulos and D. J. Nagel, Int. J. Quantum Chem. **5**, 515 (1971); D. A. Papaconstantopoulos and P. N. Poulopoulos, Solid State Commun. **41**, 93 (1982).
[6] V. E. Egorushkin and S. E. Kulkova, J. Phys. F: Met. Phys. **12**, 2823 (1982); S. E. Kulkova and V. E. Egorushkin, Solid State Commun. **77**, 667 (1991); V. N. Grishkov, S. E. Kulkova, O. N. Muryzhnikova, V. P. Lapshin, and A. I. Lotkov, Fiz. Tverd. Tela (St. Petersburg) **38**, 2631 (1996); S. E. Kulkova and O. N. Muryzhnikova, Russ. Phys. J. **7**, 123 (1996); S. E. Kulkova, D. V. Valujsky, and I. Yu. Smolin, *ibid.* **11**, 960 (1999).
[7] G. L. Zhao *et al.*, Phys. Rev. B **40**, 7999 (1989).
[8] G. Bihlmayer, R. Eibler, and A. Neckel, Ber Bunsenges. Phys. Chem. **96**, 1625 (1992); J. Phys.: Condens. Matter **5**, 5083 (1993); Philos. Mag. B **73**, 511 (1996).
[9] A. Pasturel *et al.*, Phys. Rev. B **52**, 15 176 (1995).
[10] J. M. Zhang and G. Y. Guo, J. Phys.: Condens. Matter **7**, 6001 (1995); Phys. Rev. Lett. **78**, 4789 (1997).
[11] M. Sanati, R. C. Albers, and F. J. Pinski, Phys. Rev. B **58**, 13 590 (1998).
[12] H. J. Liu and Y. Y. Ye, Solid State Commun. **106**, 197 (1998).
[13] T. Fukuda and T. Kakeshita, Mater. Sci. Eng., A **273-275**, 166 (1999).
[14] J. Cai *et al.*, Phys. Rev. B **60**, 15 691 (1999).
[15] *Biocompatibility of Clinical Implant Materials*, edited by D. Williams (CRC Press, Inc., Boca Raton, FL, 1981).
[16] V. E. Gunter, *Shape-Memory Effects and its Application in Medicine* (Nauka, Novosibirsk, 1992).
[17] S. A. Shabalovskaya, J. Phys. IV **5**, C8-1199 (1995).
[18] R. P. Hausinger, *Biochemistry of Nickel* (Plenum Press, New York, 1993).
[19] D. G. Dempsey, L. Kleinman, and E. Caruthers, Phys. Rev. B **13**, 1489 (1976).
[20] C. L. Fu and A. J. Freeman, Phys. Rev. B **33**, 1755 (1986); J. Magn. Magn. Mater. **69**, L1 (1987); Chun Li, A. J. Freeman, and C. L. Fu, *ibid.* **75**, 53 (1988).
[21] M. F. Onellion *et al.*, Phys. Rev. B **33**, 7322 (1986).
[22] J. Spisak and J. Hafner, J. Phys.: Condens. Matter **11**, 6359 (1999).
[23] R. Pencheva and M. Scheffler, Phys. Rev. B **61**, 2211 (2000).
[24] M. Eder, J. Hafner, and E. G. Moroni, Phys. Rev. B **61**, 11 492 (2000).
[25] G. Bihlmayer, T. Asada, and S. Blugel, Phys. Rev. B **62**, 11 937 (2000).
[26] S. V. Man'kovski and V. T. Cherepin, Metallofiz. Noveishie Tekhnol. **19**, 57 (1997).
[27] Yu. M. Koroteev, A. G. Lipnitskii, E. V. Chulkov, and I. I. Naumov, Phys. Low-Dimens. Struct. **9/10**, 85 (1998); **5/6**, 175 (1999).
[28] F. Amalou, M. Benakki, A. Mokrani, and C. Demangeat, Eur. Phys. J. B **9**, 149 (1999).
[29] M. Talanana *et al.*, Eur. Phys. J. B **22**, 497 (2001).
[30] J. Lee, C. Fu, and A. Freeman, Phys. Rev. B **36**, 9318 (1987).
[31] S. Lui *et al.*, Phys. Rev. B **42**, 1582 (1990).
[32] B. Hammer and M. Scheffler, Phys. Rev. Lett. **74**, 3487 (1995).
[33] S. V. Man'kovski, A. A. Ostroukhov, V. V. Flok, and V. T. Cherepin, Metallofiz. Noveishie Tekhnol. **18**, 57 (1996).
[34] G. Bihlmayer, R. Eibler, and R. Podloucky, Surf. Sci. **402-404**, 794 (1998); **446**, 188 (2000).
[35] M. Weinert, E. Wimmer, and A. J. Feeman, Phys. Rev. B **26**, 4571 (1982).
[36] P. Blaha, K. Shwartz, and J. Luits, *WIEN97, A Full Potential Linearized Augmented Plane Wave Package for Calculating Crystal Properties* (Karlheinz Schwarz, Techn. Univ., Vienna, 1999) [updated Unix version of P. Blaha, K. Schwartz, P. Sorantin, and S. B. Trickey, Comput. Phys. Commun. **59**, 399 (1990)].
[37] E. A. Brandes and G. B. Brook, *Smithells Metals Reference Book*, 7th ed. (Butterworth-Heinemann, London, 1992).
[38] I. E. Tamm, Zh. Eksp. Teor. Fiz. **3**, 34 (1933).
[39] W. Shockley, Phys. Rev. **56**, 317 (1939).
[40] D. E. Eastman, Phys. Rev. B **2**, 1 (1970).
[41] J. P. Perdew, S. Burke, and M. Ernzerhof, Phys. Rev. Lett. **77**, 3865 (1996).
[42] V. V. Nemoshkalenko, *Rentgenovskaya Emissionnaya Spectroscopiya Metallov i Splavov* (Naukova Dumka, Kiev, 1972).
[43] I. I. Sasovskaya, Fiz. Met. Metalloved. **50**, 977 (1980); **69**, 72 (1990); Phys. Status Solidi B **164**, 327 (1991).
[44] Joo Yull Rhee, B. N. Harmon, and D. W. Lynch, Phys. Rev. B **54**, 17 385 (1996); **59**, 1878 (1999).